Modulated Fourier expansions and Heterogeneous Multiscale Methods

J. M. Sanz-Serna
Departamento de Matemática Aplicada,
Universidad de Valladolid, Spain
sanzsern@mac.uva.es
hermite.mac.cie.uva.es/sanzserna

Version: 8 April 2008

Dedicated to Arieh Iserles on his sixtieth birthday

Abstract

We show that, for highly-oscillatory ordinary differential equations problems, the modulated Fourier expansion approach can be advantageously used to understand and analyze the Heterogenous Multiscale Methods introduced by E, Engquist and their co-workers.

1 Introduction

Heterogenous Multiscale Methods (HMMs) provide a general methodology for the numerical simulation of systems with widely different scales. Their aim is 'to capture the macroscale behavior of the system with a cost that is much less than the cost of full microscale solvers' and they consist of a 'macroscale solver and a procedure for estimating the missing numerical data from the microscale model' (E *et al.* 2007). They were introduced by E & Engquist 2003 and may be applied in very different fields; an extensive survey has been provided by E *et al.* 2007. Here we focus on HMMs as applied to highly-oscillatory ordinary differential equations (E 2003, Engquist & Tsai 2005, Sharp *et al.* 2005, Ariel *et al.* 2008, cf. Li *et al.* 2007) and show how the analysis of these algorithms may benefit from the use of modulated Fourier expansions.

Modulated Fourier expansions, i.e. Fourier expansions where the amplitudes of the Fourier modes do not remain constant but vary slowly, are a very common tool throughout Applied Mathematics. In Numerical Analysis they were first employed by Hairer & Lubich 2000 and their application is gaining momentum, as witnessed by the list of references in the monograph by Hairer *et al.* 2006.

Even though the modulated Fourier expansion approach to the analysis of HMMs possesses a wide applicability, we have preferred to restrict this short article to a single

case study: the inverted pendulum. In 1908 the physicist Stephenson showed experimentally that an inverted pendulum (i.e. a pendulum where the rod is directly above the pivot) will not fall down if the pivot is subjected to vertical vibrations of small amplitude and sufficiently high frequency. Stephenson's discovery has spawned in impressive body of physical and mathematical literature that includes Nobel-prize-winning work (see e.g. Levi 1999, Sanz-Serna 2008b). There are at least two factors that render the inverted pendulum a good model for the application of HMMs. The most obvious reason is that in the inverted pendulum the fast vibration of the pivot (microscale), in spite of being of a possibly very small amplitude, influences substantially the motion of the bob. In fact, the macroscale effect is so large that gravity is overcome and the bob is prevented from falling down. On the other hand, in the inverted pendulum the connection between the macroscale and microscale variables is more complicated than in other systems (the angular velocity of the macroscale bob motion may be widely different from the instantaneous angular velocity). It is likely that these reasons led Engquist and his co-workers to consider in detail the application of HMMs to the inverted pendulum (Sharp *et al.* 2005, see also Ariel *et al.* 2008). Their analysis of the numerical technique is built on the analytical study of the pendulum provided by Levi 1999 and based on the method of averaging (i.e. essentially in the iteration of changes of variables to reduce the full dynamics of the system to the dynamics of a set of slowly varying, averaged variables). Here, as in several recent contributions by Hairer, Lubich and their co-workers, changes of variables are avoided and, alternatively, modulated Fourier expansions are used to identify the slow variables and the corresponding (macroscale) differential equations. The estimates in this paper are stronger than those in Levi 1999 or Sharp *et al.* 2005 (but this does not necessarily imply that our estimates cannot be derived via changes of variables).

This article has been divided into five sections. Section 2 presents the inverted pendulum equations and the corresponding modulated Fourier expansions. The numerical algorithm is described in Section 3 and analyzed, in a straightforward manner, in Section 4. Numerical experiments are presented in the final section that, once more, clearly show that the HMMs are capable of finding accurately the macroscale dynamics of the pendulum with a low computational cost. In fact, it turns out that, in a relevant parameter range, the HMM algorithm employed here provides $O(H^2)$ approximations uniformly in the pivot frequency.

2 Modulated Fourier expansions

2.1 Problem specification

Our starting point is the pendulum equation

$$\frac{d^2q}{dt^2} = \ell^{-1} g \sin q,$$

where $g > 0$ is the acceleration of gravity, ℓ denotes the pendulum length and q measures the angle between the *upward* vertical axis and the rod; we are primarily interested in the behavior near the unstable top-most equilibrium at $q = 0$. When the pivot

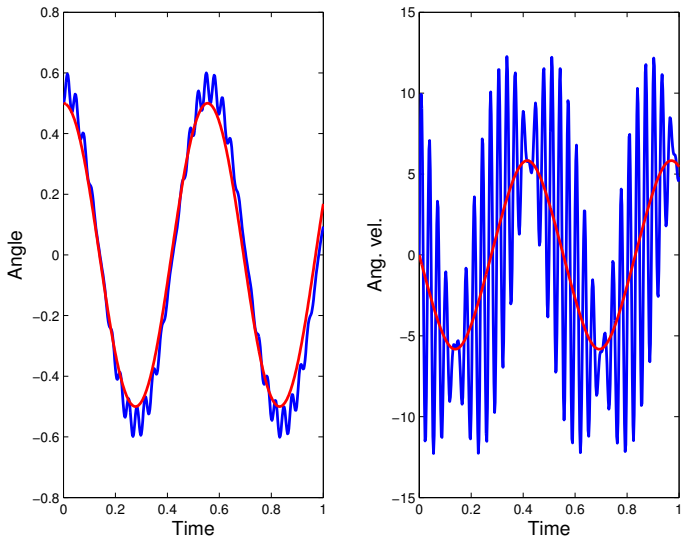

Figure 1: Behavior of q and dq/dt for $\omega = 200$

of the pendulum is subjected to a vertical acceleration $a(t)$, the equation of motion becomes

$$\frac{d^2q}{dt^2} = \ell^{-1}(g + a(t)) \sin q. \tag{1}$$

(Here $a(t) > 0$ when the acceleration is upwards.) We focus on the simplest choice where $a(t)$ is sinusoidal; in this case, we write

$$a(t) = v_{max}\, \omega \cos \omega t; \tag{2}$$

$v_{max} > 0$ measures the maximum value of the velocity $v(t) = v_{max} \sin \omega t$ of the pivot and $\omega \gg 1$ is the 'large' parameter in the perturbation analysis that follows. Thus, with respect to this parameter, $a(t)$ is an $O(\omega)$ quantity, while $v(t) = O(1)$. It is well known (and will be proved below), that, for fixed initial conditions, the solution $q(t)$ of (1) behaves as the superposition of an *'averaged' solution,* that varies slowly, and a rapid oscillation with frequency $O(\omega)$ and small, $O(\omega^{-1})$, amplitude. For the angular velocity dq/dt, the superimposed fast oscillation has $O(1)$ amplitude. This behavior is illustrated in Fig. 1, where ω has the moderate value 200 (larger values of the parameter, like those used in the numerical experiments below, give a blurred picture for dq/dt and a smooth cosine-like curve for q).

For the analysis, in lieu of (1)–(2), we consider the more general format

$$\frac{d^2q}{dt^2} = (a_0 + a_1 \omega e^{i\omega t} + cc) f(q),$$

or, equivalently,

$$\frac{dp}{dt} = (a_0 + a_1 \omega e^{i\omega t} + cc) f(q), \qquad \frac{dq}{dt} = p, \tag{3}$$

where q are f are real vectors, a_0 is a real constant, a_1 a complex constant, ω is a positive parameter and the short-hand notation cc means 'complex conjugate of the preceding term.' Many extensions of (3) may be treated without much additional effort, but we are not interested in them here.

2.2 Formal expansions

The modulated Fourier expansion ansatz for the solutions of (3) is given by

$$\begin{aligned} p(t) &= P(t) + w^{(1)}(t)e^{i\omega t} + cc + w^{(2)}(t)e^{i2\omega t} + cc + \cdots, \quad (4)\\ q(t) &= Q(t) + z^{(1)}(t)e^{i\omega t} + cc + z^{(2)}(t)e^{i2\omega t} + cc + \cdots, \quad (5) \end{aligned}$$

where the 'averaged' variables P, Q and the *modulation functions* $w^{(k)}$, $z^{(k)}$ are bounded, along with all their derivatives, independently of ω. Furthermore, $P, Q = O(1)$, $w^{(k)} = O(\omega^{-k+1})$, $z^{(k)} = O(\omega^{-k})$, $k = 1, 2, \ldots$ (compare with the behavior borne out in Fig. 1) and, in view of the second equation in (3), we take at the outset

$$\frac{dQ}{dt} = P. \quad (6)$$

The modulation functions may be determined recursively in a step-by-step fashion.

First step. We begin by taking the ansatz (4)–(5) to the first equation in (3) to get

$$i\omega w^{(1)}e^{i\omega t} = a_1\omega e^{i\omega t}f(Q) + O(1).$$

Therefore, we may write

$$w^{(1)} = -ia_1 f(Q) + O(\omega^{-1}), \quad (7)$$

so that, at leading order, the component of frequency ω in the angular velocity p is 'enslaved' to the slow variation of the angle q.

Second step. We now use (7) in (4) and then substitute the ansatz (4)–(5) in the second equation of (3) and obtain

$$\frac{dQ}{dt} + i\omega z^{(1)}e^{i\omega t} = P - ia_1 f(Q)e^{i\omega t} + O(\omega^{-1}).$$

By equating the terms involving $e^{i\omega t}$, we find the enslavement, at leading order, of $z^{(1)}$ to Q,

$$z^{(1)} = -\omega^{-1}a_1 f(Q) + O(\omega^{-2}). \quad (8)$$

Third step. We turn again to the first equation in (3). Substitution of the ansatz (4)–(5), with (7) and (8) taken into account, yields, by equating the terms involving $e^{i1\omega t}$, $e^{i2\omega t}$, the $O(\omega^{-1})$ components of the fast variation of p. After completion of the third step, the ansatz reads

$$\begin{aligned} p &= P + [-ia_1 f(Q) + \omega^{-1}a_1 f'(Q)P + \cdots]e^{i\omega t} + cc\\ &\quad + \frac{i}{2}\omega^{-1}a_1^2 f'(Q)f(Q)e^{i2\omega t} + cc + \cdots, \quad (9)\\ q &= Q + [-\omega^{-1}a_1 f(Q) + \cdots]e^{i\omega t} + cc + \cdots. \quad (10) \end{aligned}$$

n-th step. The procedure we are following may be iterated to determine all modulation functions in (4)–(5) as formal power series in ω^{-1} with coefficients given by functions of P and Q. The vector expressions $f(Q)$, $f'(Q)P$, $f'(Q)f(Q)$, ... that appear in (9)–(10) clearly coincide with the familiar elementary differentials for the system $dP/dt = f(Q)$, $dQ/dt = P$, as found in the analysis of Runge-Kutta-Nyström methods (Hairer *et al.* 1993, II.14, Sanz-Serna & Calvo 1994, 4.6). By using this observation, it would not be difficult to obtain a general expression for the modulation functions; however such a task would lead us astray and will not be pursued here.

Modulated expansion for the force. Differentiation of (4) with respect to t leads to the modulated Fourier expansion for the force dp/dt:

$$\frac{dp}{dt} = \frac{dP}{dt} + [a_1 \omega f(Q) e^{i\omega t} + cc] - [a_1^2 f'(Q) f(Q) e^{i2\omega t} + cc] + \cdots . \qquad (11)$$

Differential equation for P. Once the modulation functions, to any desired order in ω^{-1}, have been determined in terms of the averaged P and Q, we carry the ansatz to the first equation in (3) and retain the non-oscillatory component to obtain a differential equation for P. At leading order, one finds:

$$\frac{dP}{dt} = a_0 f(Q) - 2|a_1|^2 f'(Q) f(Q) + O(\omega^{-2}). \qquad (12)$$

2.3 Bounds

We now employ the preceding formal results to obtain rigorous estimates for the difference between the solutions of the system (3) we wish to integrate and solutions of the *averaged* system

$$\frac{dP}{dt} = a_0 f(Q) - 2|a_1|^2 f'(Q) f(Q), \qquad \frac{dQ}{dt} = P, \qquad (13)$$

obtained by discarding the $O(\omega^{-2})$ remainder in (12).

Theorem 1 *Consider the IVP on $0 \le t \le T < \infty$ given by*

$$p(0) = p_0, \quad q(0) = q_0, \qquad (14)$$

and (3), where f is assumed to be sufficiently smooth. Then

$$p(t) = P(t) - i a_1 e^{i\omega t} f(Q(t)) + cc + R_p(t), \qquad (15)$$

$$q(t) = Q(t) + R_q(t), \qquad (16)$$

where P and Q solve (13) with initial conditions

$$P(0) = p_0 + i a_1 f(q_0) + cc, \qquad Q(0) = q_0, \qquad (17)$$

and, for $\omega > \omega_0$, the remainder functions R_p and R_q have bounds of the form $C\omega^{-1}$. Here ω_0 and C are constants independent of t and ω (that may depend on f, a_0, a_1, p_0, q_0, T).

Proof. The idea is to use the truncation of (9)–(10) given by

$$\begin{aligned} p_* &= P + [-ia_1 f(Q) + \omega^{-1} a_1 f'(Q) P] e^{i\omega t} + cc \\ &\quad + \frac{i}{2} \omega^{-1} a_1^2 f'(Q) f(Q) e^{i2\omega t} + cc, \\ q_* &= Q + [-\omega^{-1} a_1 f(Q)] e^{i\omega t} + cc, \end{aligned}$$

with P and Q as in the statement of the theorem, and bound $p - p_*$ and $q - q_*$ by a Gronwall-lemma argument. Care should be exercised due to the $O(\omega)$ Lipschitz constant in the first equation of the system (3).

We change dependent variables $(p, q) \to (m, q)$, with

$$m = p + (ia_1 e^{i\omega t} + cc) f(q) \tag{18}$$

(a physical interpretation is given in Sanz-Serna 2008b); the equations (3) become

$$\frac{dm}{dt} = a_0 f(q) + (ia_1 e^{i\omega t} + cc) f'(q) m - (ia_1 e^{i\omega t} + cc)^2 f'(q) f(q), \tag{19}$$

$$\frac{dq}{dt} = m - (ia_1 e^{i\omega t} + cc) f(q); \tag{20}$$

a system whose Lipschitz constant is $O(1)$. If we define

$$m_* = p_* + (ia_1 e^{i\omega t} + cc) f(q_*), \tag{21}$$

then the functions m_* and q_* satisfy (19)–(20) up to an $O(\omega^{-1})$ residual and the result follows from the standard Gronwall lemma.

By using (15)–(16), it is then possible to express, except for an $O(\omega^{-1})$ error, the solution of the initial value problem (3), (14) in terms of the 'easier' initial value problem (13), (17). We emphasize that P by itself does not provide an $O(\omega^{-1})$ approximation to p and that the initial values for p and P are different. The result by Levi 1999 on which the analysis by Sharp *et al.* 2005 is based has a weaker, $O(\omega^{-1/2})$, estimation rather than $O(\omega^{-1})$.

We shall also use a rigorous result in connection with the formal expansion of the force found in (11):

Theorem 2 *In the situation of the preceding theorem,*

$$\frac{dp}{dt} = \frac{dP}{dt} + [a_1 \omega f(Q) e^{i\omega t} + cc] - [a_1^2 f'(Q) f(Q) e^{i2\omega t} + cc] + R_f, \tag{22}$$

where, for $\omega > \omega_0$, the remainder functions R_f has a bound of the form $C_f \omega^{-1}$. Here ω_0 and C_f are constants independent of t and ω (that may depend on f, a_0, a_1, p_0, q_0, T).

Proof. Use (18) (resp. (21)) to express the derivative dm/dt in terms of p and q (resp. the derivative dm_*/dt in terms of P and Q) and note that, by (19), these two derivatives differ by terms of size $O(\omega^{-1})$.

2.4 Stabilization by vibration

The force in the averaged system (13) differs from the force in (3) in that the $O(\omega)$ oscillatory terms have disappeared and, furthermore, in the appearance of an extra $O(1)$ contribution given by $-2|a_1|^2 f'(Q)f(Q)$. In the particular case of the pendulum (1)–(2), the extra contribution reads $-[v_{max}^2/(2\ell)]\cos Q \sin Q$. Near the top-most $Q = 0$ position, this extra force opposes the gravitational force $(g/\ell)\sin Q$ in the standard pendulum equation; for $v_{max}^2 > 2\ell g$ the extra force overcomes gravitation and $Q = 0$ becomes a *stable* equilibrium of the averaged system

$$\frac{dP}{dt} = \left(\frac{g}{\ell} - \frac{v_{max}^2}{2\ell}\cos q\right)\sin q, \qquad \frac{dQ}{dt} = P.$$

This observation is the key in deriving stability results for the the inverted pendulum equation (1) (Levi 1999, Sanz-Serna 2008b).

3 Heterogeneous Multiscale Methods

In this Section it is convenient to rewrite the system (3) and the averaged system (13) in the compact forms respectively given by

$$\frac{dp}{dt} = \phi(q, \omega t; \omega), \;\; \phi(q, \tau + 2\pi, \omega) \equiv \phi(q, \tau, \omega), \qquad \frac{dq}{dt} = p \tag{23}$$

and

$$\frac{dP}{dt} = \Phi(Q), \quad \frac{dQ}{dt} = P. \tag{24}$$

For simple model problems, including the pendulum, it is perfectly feasible, given (23), to determine *analytically* the averaged system (24) and then to perform a numerical integration of the latter with a step-length H dictated by the rate of variation of the averaged solutions and independent of ω. Such numerical integration will be referred to as a *macrointegration*; H is the corresponding *macrostep-size*. The HMM can be thought of as a method to perform a macrointegation without using explicit knowledge of the force Φ, thus bypassing the need to carry out analytically the process of averaging.

In the HMM, the values of Φ required by the macrointegrator are found as numerical averages of values of $\phi(q, \omega t; \omega)$; these averages are obtained with the help of a *filter* function K. In turn, the values of q that feature among the arguments of the vectors $\phi(q, \omega t; \omega)$ being averaged are computed by numerically integrating the original system (23). These auxiliary numerical integrations are called *microintegrations*.

The overall HMM thus depends on the choices of macrointegrator, filter and microintegrator. To simplify the exposition, we restrict the attention to a single, simple choice for each of these three elements.

3.1 Macrointegration

The macrointegration is carried out with the well-known Verlet scheme, so that the step from $t_n = nH$ to $t_{n+1} = t_n + H$ reads:

$$P_{n+1/2} \;\; = \;\; P_n + \frac{H}{2}\Phi_n,$$

$$\begin{aligned} Q_{n+1} &= Q_n + HP_{n+1/2}, \\ P_{n+1} &= P_{n+1/2} + \frac{H}{2}\Phi_{n+1}. \end{aligned}$$

Here Φ_n is an approximation to $\Phi(Q_n)$ and, of course, the starting P_0, Q_0 are taken from (17).

3.2 Filter

If K is given by (Engquist & Tsai 2005)

$$K(\xi) = C \exp\left(\frac{5}{\xi^2 - 1}\right), \quad -1 < \xi < 1,$$

with C chosen so that

$$\int_{-1}^{1} K(\xi)\, d\xi = 1,$$

the forces Φ_n required by the macro-integrator are obtained through the convolution

$$\Phi_n = \frac{2}{\eta} \int_{t_n - \eta/2}^{t_n + \eta/2} K\left(\frac{s - t_n}{\eta/2}\right)\ \phi(q^n(s), \omega s; \omega)\ ds, \tag{25}$$

where $\eta > 0$ is a scale factor and q^n, to be discussed later, is an approximation to the solution q of (23).

To gain some insight into the process of filtering, note first that for

$$\psi(t) = \Psi(t) \exp(ik\omega t),$$

with Ψ slowly varying and $k \neq 0$, the output of the filter

$$\frac{2}{\eta} \int_{t_n - \eta/2}^{t_n + \eta/2} K\left(\frac{s - t_n}{\eta/2}\right)\ \psi(s)\ ds, \tag{26}$$

will be small: the positive and negative lobs of (the real or imaginary parts of) the integrand cancel in the integration. On the other hand, for ψ slowly varying and η small, (26) is an $O(\eta^2)$ approximation to $\psi(t_n)$. Now Theorem 2 along with (23)–(24) show that $\phi(q, \omega s; \omega)$ is composed of (i) $\Phi(Q)$, (ii) rapidly oscillatory components and (iii) the $O(\omega^{-1})$ reminder R_f. The rapid oscillations will hopefully be annihilated by the filter and therefore (25) is expected to approximate $\Phi(Q(t_n))$.

We remark that similar filters (there called weight functions) are used by the Mollified Impulse Method (García-Archilla *et al.* 1998, Sanz-Serna 2008a) in order to suppress the rapidly oscillatory components of the force. However the Mollified Impulse Method does not qualify as an HMM because it builds up complete knowledge of the microscale.

3.3 Microintegration

Assume that, in macrointegration step $n-1 \to n$, $n \geq 1$, we have found $P_{n-1/2}$, Q_n and are ready to use (25) to determine the force value Φ_n to be employed in the computation of P_n that closes the step (the same value of the force is used again at the beginning of the next step $n \to n+1$). We compute a prediction

$$\hat{P}_n = P_{n-1} + H\Phi_{n-1},$$

based on available information, and define q^n through the initial value problem given by the original system (23) along with the initial data (cf. Theorem 1)

$$p^n(t_n) = \hat{P}_n - ia_1 \exp(i\omega t_n) f(Q_n) + cc, \quad q^n(t_n) = Q_n. \tag{27}$$

(At $n = 0$, this formula is used with $\hat{P}_0 = P_0$.)

In practice, the integral in (25) has to be replaced by a quadrature rule. In our experiments, we apply the trapezoidal rule on a fine uniform grid obtained by dividing the interval $[t_n - \eta/2, t_n + \eta/2]$ into subintervals of length h. The values of q^n at the points of the fine grid are obtained by a *microintegration* of the original system (23) with initial condition (27) through the Verlet algorithm with (micro)step-length h. (In fact, at each t_n the microintegration requires a forward leg from t_n to $t_n + \eta/2$ and a backward leg from t_n to $t_n - \eta/2$.)

4 Analysis

We now discuss the behavior of the errors in the algorithm. We consider a_0, a_1 and f in the differential equation, the initial conditions p_0 and q_0 and the integration interval $0 \leq t \leq T$ as *fixed* and study the effect of changing the values of the parameters ω, H, η, h.

We begin by noticing that the error consists of an $O(\omega^{-1})$ *averaging error* introduced by approximating the true solution (p, q) by means of the averaged (P, Q) through formulas (15)–(16) in Theorem 1 and a *numerical error* resulting by replacing $(P(t_n), Q(t_n))$ by the numerical approximations (P_n, Q_n).

In turn, the numerical error is of course the global error in the application to the averaged system of the Verlet algorithm with step-size H and inexact force values Φ_n. By means of a standard stability plus consistency analysis of the Verlet method, it follows that

$$\max_n \left(||P_n - P(t_n)|| + ||Q_n - Q(t_n)|| \right) = O(H^2 + \epsilon) \tag{28}$$

where the term H^2 stems from the local truncation error and

$$\epsilon = \max_n |\Phi(Q(t_n)) - \Phi_n^*|$$

bounds the differences between the exact forces $\Phi(Q(t_n))$ and the values Φ_n^* that the algorithm would use if the computation of the forces Φ_n *started from data* $P(t_n)$,

$Q(t_n)$ *taken from the exact averaged solution*. The different sources of error that build up ϵ will now be discussed successively.

Effect of the filter. Consider (25) with q^n equal to the exact q and recall the discussion around formula (26). The function being filtered differs from $\Phi(Q)$ in rapidly oscillatory components and in an $O(\omega^{-1})$ residual. The filter reproduces the slowy varying $\Phi(Q)$ except for an $O(\eta^2)$ error. For the rapidly oscillatory components (of size $O(\omega)$), we integrate by parts an arbitrary number m of times. The boundary contributions are zero, because the filter function K vanishes with all its derivatives at $\xi = \pm 1$, and each integration introduces in the integral a factor $(\eta\omega)^{-1}$. Thus the filter annihilates the oscillatory components except for an $O(\omega(\eta\omega)^{-m})$ residual. Summing up, the error originating from the filter is then (cf. Engquist & Tsai 2005, Theorem 2.5)

$$\epsilon_{filter} = O(\eta^2 + \omega(\eta\omega)^{-m} + \omega^{-1}).$$

Effect of the quadrature rule. Standard results for the trapezoidal rule on a partition of diameter h of an interval of length η show this effect to be

$$\epsilon_{quad} = O(\eta h^2 \omega^3).$$

The factor ω^3 corresponds to the size of the second derivative of the force ϕ with respect to time.

Effect of the microintegration. The investigation of the error induced by the microintegration is rendered easier if, for the analysis, the system (23) is rewritten in terms of the new time variable $\tau = \omega t$, so that corresponding Lipschitz constant is reduced from $O(\omega)$ to $O(1)$. Then each microintegration leg spans an interval $0 \leq \tau \leq \eta\omega/2$ and is performed with a step-size ωh. Since the derivatives of q with respect to τ are $O(\omega^{-1})$, the errors in q are of the order of $\chi(\eta\omega)(\omega h)^2\omega^{-1}$ and they will originate errors

$$\epsilon_{micro} = O(\chi(\eta\omega)(\omega h)^2)$$

in the function ϕ in (25) that has an $O(\omega)$ Lipschitz constant. Here $\chi(\eta\omega)$ is a constant whose value depends on the product $\eta\omega$; the exact functional dependence will vary with the system being integrated. Often, global errors in oscillatory problems grow linearly with time and in those cases χ will be proportional to $\eta\omega$, but worse rates of growth are of course also common.

Effect of the predictor. The Euler-like predictor clearly introduces a perturbation

$$\epsilon_{pred} = O(H^2).$$

This concludes our straightforward error analysis, that may be compared with that provided by Sharp *et al.* 2005.

In the numerical experiments to be reported in the next section, we have used the following approach. We write $\eta = M(\omega/2\pi)$, so that, at each t_n, the microintegration spans M fast periods, and determine the integer M so as to have a negligible filtering error (for the given problem and for a given range of the values of the parameters ω, h, H). Too large a value of M results in inaccuracies due to the smearing of the slow-varying component of the force and if M is too small the rapid oscillations will not be filtered out. With M fixed, η is no longer a free parameter. Furthermore, we

H	HMM				Averaged
	Microsteps	$\omega = 10^4$	$\omega = 10^6$	$\omega = 10^8$	
1/10	4,000	4.04(-1)	4.08(-1)	4.04(-1)	2.74(-1)
1/20	16,000	1.05(-1)	1.07(-1)	1.08(-1)	7.43(-2)
1/40	64,000	2.51(-2)	2.70(-2)	2.61(-2)	1.90(-2)
1/80	256,000	4.76(-3)	6.72(-3)	6.69(-3)	4.72(-3)
1/160	1,024,000	2.80(-4)	1.68(-3)	1.65(-3)	1.18(-3)

Table 1: Errors in q for the inverted pendulum

set $H = T/N$ and $h = (\omega/2\pi)/N$, so that there are as many macrosteps in the interval $[0, T]$ as microsteps in a period of the fast oscillation (obviously one may more generally consider $h = \alpha(\omega/2\pi)/N$ with α a moderate constant). With this set-up only ω and N (or equivalently ω and H) are free parameters and the preceding analysis shows that, as long as ϵ_{filter} is negligible, then ϵ in (28) is $O(H^2)$ *uniformly in* ω. At the same time, the number of microsteps —which is a reasonable yardstick for measuring the cost of the algorithm— behaves like $O(N\eta h^{-1}) = O(N^2)$ and is thus independent of ω! Halving the errors requires halving the value of H; a behavior one associates with first-order methods.

5 Numerical results

We have applied the HMM to the inverted pendulum equations (1)–(2) when $\ell = 20cm$, $g = 9.8ms^{-2}$ and $v_{max} = 4ms^{-1}$, a choice of constants for which the period of the small (stable) oscillations near the usually unstable equilibrium $q = 0$ is $\approx 0.51s$. The initial conditions are $p_0 = 0$, $q_0 = 0.5$ and we took $T = 1$. With the approach outlined at the end of the preceding section, we found that for $M = 40$ the error arising from the filter is negligible.

Table 1 gives the maximum over $0 \leq t \leq T$ of the error $|Q_n - Q(t_n)|$ of the computed solution Q_n with respect to the exact solution of the averaged system. (The maximum over t of $|q(t) - Q(t)|$ is $\approx 20\omega^{-1}$.) The column 'Averaged' refers to the case where the Verlet integrator with step H is applied directly to the averaged system (i.e. it corresponds to $\epsilon = 0$ in (28)). As pointed out previously, ϵ_{filter} is negligible and therefore the differences between the column 'Averaged' and the three columns corresponding to the HMM are due to the effects of the microintegrations, the numerical quadratures and the predictor. The errors in the HMM possess the $O(H^2)$ behavior, uniformly in ω, established by our analysis. Indeed the HMM results displayed are hardly dependent on ω; the only exceptions corresponds to $\omega = 10^4$ and $H = 1/80$ or $H = 1/160$, where it is likely that a cancellation takes place between errors arising from different sources.

From the Table it is clear that the HMM results are comparable with those one would obtain from a macrointegration of the averaged equations; this is in agreement with the HMM concept 'integrate for the macrobehavior without knowing the corre-

sponding equation'. Let us remark that for $\omega = 10^8$ and $H = 1/20$ the HMM produces errors of size 0.1 with only 16,000 microsteps; a number three orders of magnitude smaller than the number ($\approx 1.6 \times 10^7$) of full cycles that have taken place in the vibration of the pendulum pivot. The advantages of the HMM would be more marked if the Verlet integrators were replaced by more sophisticated choices.

For values of ω significantly lower than those considered in the table (say $\omega = 10^2$), the HMM looses its appeal: the averaged system does not provide a sufficiently accurate description of the pendulum motion and furthermore a straightforward integration of the original system by any conventional method is feasible. On the other hand, the only difficulty that the HMM experiences with larger values of ω (say $\omega = 10^{10}$) comes from the use of finite precision arithmetic: the algorithm retrieves the $O(1)$ averaged force Φ essentially by subtracting $O(\omega)$ values of the true force ϕ.

Acnowledegement. My research is supported by project MTM 2007-63257, DGI, MEC, Spain.

References

[1] ARIEL, G., ENGQUIST, B. & TSAI, R. 2008 A multiscale method for highly oscillatory ordinary differential equations with resonance, *Math. Comput.* to appear.

[2] E, W. 2003 Analysis of the heterogeneous multiscale method for ordinary differential equations. *Comm. Math. Sci* **1**, 423–436.

[3] E, W. & ENGQUIST, B. 2003 The heterogeneous multiscale methods. *Comm. Math. Sci* **1**, 87–132.

[4] E, W., ENGQUIST, B., LI, X., REN, W. & VANDEN-EIJNDEN, E. 2007 The heterogeneous multiscale method: A review. *Commun. Comput. Phys.* **2**, 367–450.

[5] ENGQUIST, B. & TSAI, Y.-H. 2005 Heterogeneous multiscale methods for stiff ordinary differential equations. *Math. Comput.* **74**, 1707–1742.

[6] GARCIA-ARCHILLA, B., SANZ-SERNA, J. M. & SKEEL B. 1998 Long-time-step methods for oscillatory differential equations. *SIAM J. Sci. Comput.* **20**, 930–963.

[7] HAIRER, E. & LUBICH, CH. 2000 Long-time energy conservation of numerical methods for oscillatory differential equations. *SIAM J. Numer. Anal.* **38**, 414–441.

[8] HAIRER, E., LUBICH, CH. & WANNER. G. 2006 *Geometric Numerical Integration. Structure Preserving Algorithms for Ordinary Differential Equations* 2nd edn. Berlin: Springer.

[9] HAIRER, E., NØRSETT, S. P. & WANNER. G. 1993 *Solving Ordinary Differential Equations I. Nonstiff Problems* 2nd edn. Berlin: Springer.

[10] LEVI, M. 1999 Geometry and physics of averaging with applications. *Physica D* **132**, 150–164.

[11] LI., J., KEVREKIDIS, P. G., GEAR, C. W. & KEVREKIDIS, I. G. 2007 Deciding the nature of the coarse equation through microscopic simulations: the baby-bathwater scheme. *SIAM Rev.* **49**, 469–487.

[12] SANZ-SERNA, J. M. 2008a Mollified impulse methods for highly-oscillatory differential equations. *SIAM J. Numer. Anal.* **46**, 1040–1059.

[13] SANZ-SERNA, J. M. 2008b Stabilizing with a hammer. *Stoch. Dyn.* **8**, 45–57.

[14] SANZ-SERNA, J.M. & CALVO, M. P. 1994 *Numerical Hamiltonian Problems.* London: Chapman & Hall.

[15] SHARP, R., TSAI, Y.-H. & ENGQUIST, B. 2005 Multiple time scale numerical methods for the inverted pendulum problem. *Multiscale Methods in Science and Engineering,* Lect. Notes Comput. Sci. Eng. **44**. Berlin: Springer, pp 241–261.